CHEMICAL ENGINEERING TRANSACTIONS
VOL. 114, 2024
A publication of AIDIC
The Italian Association of Chemical Engineering
Online at www.cetjournal.it
Guest Editors: Petar S. Varbanov, Min Zeng, Yee Van Fan, Xuechao Wang

ISBN 979-12-81206-12-0; **ISSN** 2283-9216
DOI: 10.3303/CET24114045

Performance Analysis of Flat Plate Solar Collector Networks in Batch Operation Considering Scaling

Hebert G. Lugo-Granados[a,*], Lázaro Canizalez-Dávalos[a], Martín Picón-Núñez[b]

[a]Autonomous University of Zacatecas, Department of Chemical Engineering, Zacatecas, México
[b]University of Guanajuato, Department of Chemical Engineering, Guanajuato, Gto., Mexico
lugh871024@gmail.com

In this study, the batch operation of a solar system equipped with flat plate collectors, considering the effects of scaling fouling is investigated. During this process, the heat extracted from the working fluid as it leaves the collector field is combined with water in a storage tank. Subsequently, this mixture is recirculated through the solar network, repeating the cycle until the desired target temperature is attained. The duration of this process can vary based on the operating period and environmental conditions, and it may extend beyond a single day. Different network structures, which are represented by combinations of series-parallel arrangements with a fixed number of solar collectors are investigated. The objective of this study is to identify the network design that achieves the target temperature and the required thermal load in the shortest possible time, thereby positively impacting pumping costs. As a case study, a solar thermal plant with 40 collectors is analysed. The original structure of the collector field contains 4 lines, each line consists of 2 subsections connected in series, and each subsection includes 5 parallel-connected collectors (referred to as 4Lx5p-2s). The findings indicate that modifying the original structure to a 4Lx2p-5s (4 lines, 5 subsections by line connected in series each one with 2 collectors connected in parallel) arrangement achieves the thermal objective more efficiently, resulting in reduced operating costs, reducing the time to reach the desired temperature in one hour, which results in the increase of the number of batches that can be processed per year from 200 to 216. Over time, scaling builds up in the collectors, leading to increased pressure drops and reduced heat transfer capacity. It is demonstrated that under fouled conditions, an 8Lx5s arrangement yields a system with improved thermohydraulic performance as the batch time is reduced by almost 4 h and the number of batches that can be processed per year increases from 140 to 170.

1. Introduction

Figure 1a shows the typical batch operation of a flat plate solar collector system. Its performance is determined by several factors such as: solar radiation hours, collector outlet temperature, and network configuration, among others. When the working fluid is water, the system is prone to fouling due to scaling which affects its thermal and hydraulic performance with time. For a given number of collectors, the network structure can vary by adjusting the number of rows and the quantity of collectors in each row, while keeping the flow rate and total heat transfer area constant as shown in Figure 1b. Additionally, the flow distribution within the collectors for each configuration is modified. Thermal, hydraulic, and economic performance varies across different network scenarios. When collectors are set in parallel, the flow is divided, and the outlet temperature and pressure drop per row remain the same. Conversely, if collectors are placed in series, both temperature and pressure drop increase. The structure of a flat plate solar collector network comprises two key aspects: 1.- The number of collectors connected in series determines the achievable temperature. The more collectors in a series, the higher the temperature. 2.- Parallel Collector Lines: The number of parallel collector lines is adjusted based on the total thermal load required. Each line contributes to delivering heat to the process. In hydraulic terms, the pressure drops, and operational pumping costs depend on flow distribution, operation time, and collector scaling levels. This situation indicates that it is possible to find an optimal configuration that efficiently and economically achieves the desired temperature.

Paper Received: 24 May 2024; Revised: 23 August 2024; Accepted: 11 November 2024
Please cite this article as: Lugo-Granados H.G., Canizalez-Dávalos L., Picón-Núñez M., 2024, Performance Analysis of Flat Plate Solar Collector Networks in Batch Operation Considering Scaling, Chemical Engineering Transactions, 114, 265-270 DOI:10.3303/CET24114045

Research works have been published that address the design and optimization of flat-plate solar collectors and collector fields. However, there is limited information regarding the incorporation of scaling-induced fouling effects in these systems. Most research studies on solar collector network design focus on operational aspects, sizing, and optimization, without considering the effects of fouling in the design and operation of these systems. Arunachala et al. (2015) conducted an experimental study to determine the efficiency of solar collectors. The analysis considered variations in solar energy, water flow, and scaling-related fouling. They found that when the water flow decreases, the deposition of salts on the inner wall of the solar collector tube increases, resulting in a decrease in the instantaneous efficiency of the solar collector. Lugo-Granados et al. (2023) presented a study on the thermohydraulic effects generated by scaling in flat-plate solar collectors. They integrated a model that predicts scaling in thermal and hydraulic models. Solana et al. (2022) presented a dynamic techno-economic optimisation of the operation of a low-temperature (<100 °C) solar thermal plant, taking operational costs into account. Different studies aimed at improving the performance of solar collector networks have been presented by various authors. For instance, Koussa et al. (2015) analysed the effects of series-parallel arrangements in a field of flat-plate solar collectors. They concluded that the choice of configuration depends on the user's needs in terms of the required temperature level. Rashed et al. (2020) developed a mathematical model to design a solar collector network considering all possible arrangements. They found that as the inlet temperature increases, the number of collectors and branches also increases. Similarly, they determined that there is a limit to the number of parallel branches to reduce pressure drop. Stancius et al. (2020) used a network of 3 solar collectors configured in series or parallel. They developed graphs based on the thermal performance of the solar collector (thermal load vs. temperature) to select the best network arrangements. Unlike batch operation, continuous operation of solar collector networks involves operation strategies focused on temperature control and achieving greater thermal efficiency. One of these strategies focuses on managing the total flow rate to maintain a consistent outlet temperature. Another approach involves utilizing maximum volumetric flow to operate at lower temperatures, thereby enhancing the efficiency of the solar field (Shrestha et al., 2018). In batch operation, it is crucial to consider the operational cost, which has implications for the type of network arrangement that should be employed. From this perspective, incorporating cost analysis into batch operation allows us to identify the configuration that provides greater benefits. When a batch system operates with a parallel configuration, pumping costs are lower, but on the other hand, the operation time to reach the required temperature level is longer compared to a series configuration. In this study, the cost component to determine which arrangement performs better in a batch process is analysed.

2. Methodology

In the batch process shown in Figure 1a, the flow of hot water, m_f (kg/s), exits the solar collector field at a temperature T_o (°C). It is then mixed with the water stored in the storage tank, m_{st} (kg), gradually increasing its temperature, T_{st} (°C). Subsequently, the water returns to the collector field at a higher temperature, T_i (°C), to initiate a new cycle. In this way, the inlet temperature for a new cycle, T_i, is equal to the temperature of the previous cycle, T_{st}, as shown in Eq(1), where θ represents the iteration for each cycle.

$$T_{i,\theta} = T_{st,\theta-1} \tag{1}$$

The equilibrium temperature reached by the water in the storage tank after mixing with water from the solar collectors is obtained through Eq(2), where Cp (kJ/kg°C) represents the specific heat capacity of water. The subscripts 'f' and 'st' indicate the properties of the fluid in the network and in the storage tank, respectively.

$$T_{st} = \frac{\left(m_f\ Cp_f T_o\right) + m_{st}\ Cp_{st}\ T_{st,\theta-1}}{\left(m_{st}\ Cp_{st} + m_f Cp_f\right)} \tag{2}$$

The stored energy Q_{st} (kJ) depends on the amount of thermal load supplied by the solar collector field Q_u (kJ), as described by Eq(3) and Eq(4). The heat flow absorbed by the collectors, denoted as $\dot{Q}_u$ (kW), is a function of the heat removal factor F_R (Eq (6)), the plate area A_s (m^2), solar radiation I_G (W/m^2), the temperature difference between the plate and the surroundings (T_{pm}-T_a) (°C), and the absorptance and transmittance of the cover, denoted dimensionless as α_c and τ.

$$Q_{st} = m_{st}\ Cp_{st}(T_{st} - T_i) \tag{3}$$

$$Q_u = m_f\ Cp_f(T_o - T_i) \tag{4}$$

$$\dot{Q}_u = F_R A_s\left[I_G(\tau\alpha_c) - U_c\left(T_{pm} - T_a\right)\right] \tag{5}$$

$$F_R = \frac{\dot{m}_f Cp_f}{A_s\ U_c}\left[1 - e^{\frac{-A_s\ U_c F\prime}{\dot{m}_f Cp_f}}\right] \tag{6}$$

The heat removal factor (F_R) is a function of the mass flow rate $\dot{m}_f$ (kg/s), the overall heat loss coefficient Uc (W/m²°C), and the dimensionless efficiency factor of the collector, F´ described in Eq(7). Additionally, F´ depends on the dimensionless thermal effectiveness of the metal fin (F_A) as given by Eq(9), the tube spacing S (m), the inner diameter d_i (m) and outer diameter d_o (m) of the tubes, and the resistance to heat transfer from the absorber plate to the working fluid. These resistances are present at the junction between the plate and the tube, denoted as C_b (m²°C/W) and described in Eq(8). They also include the resistance due to the tube wall R_t (m²°C/W), the resistance arising from convection between the inner tube wall and the working fluid R_h (m²°C/W), and the fouling layer resistance R_s (m²°C/W), Eq(11).

$$F' = \frac{1/U_c}{S\left[\frac{1}{U_c[d_0 + F_A(S-d_0)]} + \frac{1}{C_b} + \frac{R_h}{\pi d} + \frac{R_t}{\pi d} + \frac{R_s}{\pi d_i}\right]} \tag{7}$$

$$C_b = k_b W/\gamma \tag{8}$$

Where k_b (W/m °C) is the thermal conductivity of the junction, W (m) is the width, and γ (m) is the thickness of the junction between the plate and the tube.

$$F_A = \frac{Tanh[M(S-d_0)/2]}{M(S-d_0)/2} \tag{9}$$

$$M = \sqrt{U_c/K_s\delta} \tag{10}$$

The terms Ks (W/m°C) and δ (m) represent the thermal conductivity and plate thickness, respectively and the parameter M (m^{-1}), is defined in Eq(10). Lugo-Granados and Picon-Nuñez (2017) developed a model to calculate the mass flux of $CaCO_3$ deposited on the tubes of thermal equipment, denoted as $\dot{m}_d$ (kg/m² s). This model enables the determination of the thermal resistance generated by fouling during the operation of a solar collector. The fouling thermal resistance, R_s (m² °C/W), is a function of the mass flux being removed, $\dot{m}_r$ (kg/m² s), the density ρ_f (kg/m³), and the thermal conductivity λ_f (W/m °C) of $CaCO_3$.

$$dR_s/dt = \dot{m}_d - \dot{m}_r/\rho_f\lambda_f \tag{11}$$

The pumping power ($\dot{w}$) is determined based on Eq(12) as a function of pressure drop. It is calculated as the product of volumetric flow rate $\dot{V}$ (m³/s) and pressure drop ΔP (kPa), divided by the pump efficiency (η_b).

$$\dot{w} = \dot{V}\,\Delta P/\eta_b \tag{12}$$

Eq(13), represents the operating cost ($Cost_b$) and indicates that they are directly proportional to the unit cost of electrical energy ($Cost_u$), the pumping power (w), and the operating time (t). In this work, the cost of electrical energy is assumed to be $0.3 USD/kWh.

$$Cost_b = Cost_u \cdot w \cdot t \tag{13}$$

3. Results

A food thermal dehydration plant installed in the city of Zacatecas, Mexico, is used as a case study (García-Valladares, 2019). The solar field consists of 40 conventional flat-plate collectors. In Figure 1a, a general diagram of the solar system is shown. The original collector field arrangement has 4 lines, with each line consisting of 2 subsections connected in series, and each subsection containing 5 collectors connected in parallel (denoted as 4Lx5p-2s). The number of lines and the quantity of collectors per line can be modified to obtain different network arrangements. Various arrangements are proposed while maintaining the total number of collectors. In Figure 1b, several possible arrangements are presented. The letters “L”, “p”, and “s” correspond to line, parallel, and series, respectively.

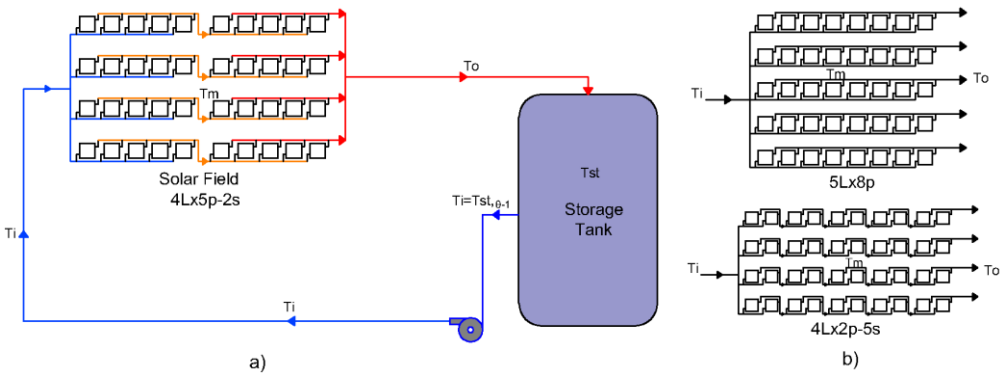

Figure 1: a) Solar batch system diagram, b) Different solar collector field arrangements

In the context of the study, the initial and target temperatures are set at 25 °C and 90 °C, respectively. The total volumetric flow rate entering the network is 80 L/min. For each configuration, the volumetric flow rate circulating through each line and collector varies. The storage tank has a capacity of 6,000 litres. Solar radiation in a typical day in September in the city of Zacatecas, Mexico, is considered. To calculate the total operating cost, the pumping cost is combined with the annualised cost of the 40 collectors, estimated at $3,247.06.
The operation of different network structures is considered. The results of the water temperature level reached in the storage tank over the course of a day are shown in Figure 2a. These results are obtained considering that scaling has been generated in the system after one year of operation. It is observed that none of the configurations reach the target temperature (90 °C) on the first day of operation. The 4Lx10s arrangement achieves the highest temperature (70 °C). To achieve the target temperature, it is necessary to operate for a second day, using the maximum temperature reached on the first day as the inlet temperature. Only the 4Lx10s and 5Lx8s arrangements achieve the target temperature on the second day of operation as shown in Figure 2b.

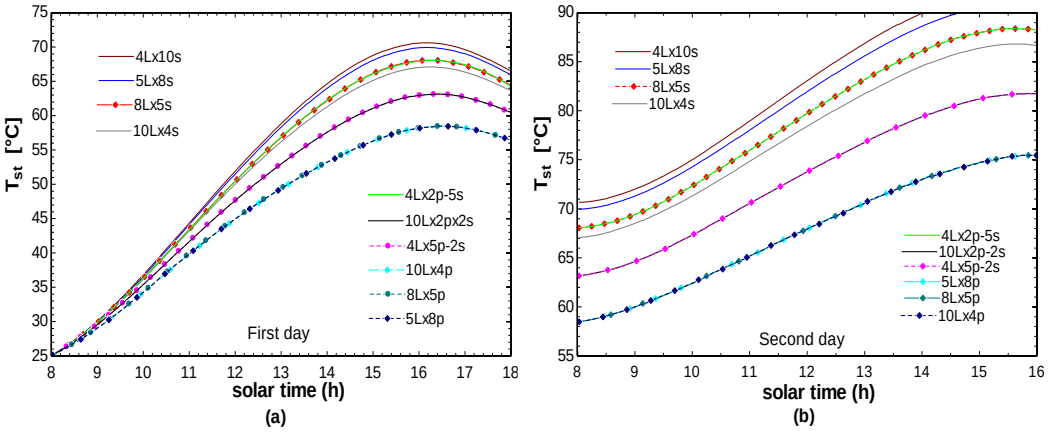

Figure 2: T*emperature profiles for the storage tank with fouling relative to solar time: (a) Start of operation, (b) Second day of operation.*

On the third day of operation, the inlet temperature corresponds to the maximum temperature reached on the second day (see Figure 3a). During the third day, the following configurations achieve the target temperature: 4Lx2p-5s, 8Lx5s, 10Lx4s, 10Lx2p-2s, and 4Lx5p-2s. However, the 5Lx8p, 8Lx5p, and 10Lx4p configurations reach the target temperature by the fourth day of operation (see Figure 3b). Notably, arrangements with the same flow distribution per collector exhibit similar behaviour. Configurations with a volumetric flow rate per collector below 2 l/min take longer to reach the target temperature, in contrast to those with higher flow rates. For the second and third days of operation, the system begins operating at 8:30 a.m. so that there is enough solar radiation to avoid heat loss during the initial cycles (refer to Figure 3a for the 4Lx2p-5s, 8Lx5s, and 10Lx4s configurations).

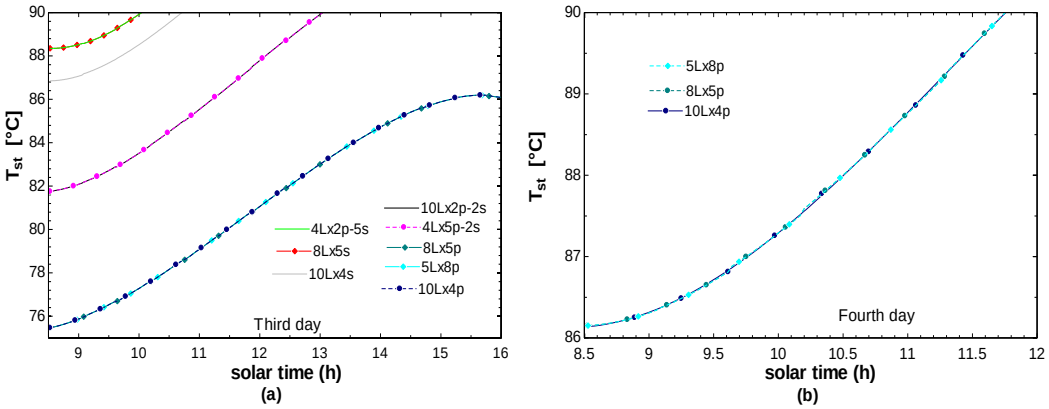

Figure 3: Temperature profiles relative to solar time: a) Third day of operation b) Fourth day of operation

For the sake of comparison, the operating costs with and without scaling are calculated. Table 1 presents the operating costs for different configurations, without considering scaling. The original arrangement (4Lx5p-2s) achieves the target temperature in 14.37 h and incurs a total cost of $3,977.23 USD/y. Meanwhile, the 4Lx10s configuration reaches the target temperature in a shorter time (13.03 h), but it generates the highest cost

($4,161.29 USD/y). On the other hand, the 4Lx2p-5s arrangement takes 13.32 h and has the lowest total cost ($3,955.94 USD/y). These findings suggest that the modification of the original configuration can enhance the solar system performance in terms of both time and operating costs.

Table 1: Operating costs of different network structures. Results without considering fouling

Arrangement	$\dot{V}$ (l/min)	ΔP (kPa)	Cost_colec (USD/y)	Cost_pump (USD/y)	Cost_Total (USD/y)	Q (kWh)	Cost_Q (USD/kWh)	Operation time (h)	Batches /y	Cost per batch (USD)
8Lx5p	2	299.8	3,247.059	911.77	4,158.83	163,020	0.0255	18	160	26.0
10Lx 2p-2s	4	300.7	3,247.059	730.17	3,977.23	163,020	0.0243	14.37	200	19.8
4Lx5p-2s	4	300.7	3,247.059	730.17	3,977.23	163,020	0.0243	14.37	200	19.8
5Lx8p	2	299.8	3,247.059	911.77	4,158.83	163,020	0.0255	18	160	26.0
4Lx2p-5s	10	314.9	3,247.059	708.88	3,955.94	163,020	0.0242	13.32	216	18.3
10Lx4p	2	299.8	3,247.059	911.77	4,158.83	163,020	0.0255	18	160	26.0
10Lx4s	8	307.6	3,247.059	709.59	3,956.65	163,020	0.0242	13.65	211	18.8
8Lx5s	10	314.9	3,247.059	720.59	3,967.65	163,020	0.0243	13.54	213	18.7
5Lx8s	16	359.9	3,247.059	797.20	4,044.26	163,020	0.0248	13.11	220	18.4
4Lx10s	20	415.3	3,247.059	914.24	4,161.29	163,020	0.0255	13.03	221	18.8

It is observed that arrays with the same flow distribution per collector exhibit similar behaviour, such as the arrays (8Lx5p, 5Lx8p, and 10Lx4p). The flow rate per collector in these arrays is 2 l/min, with an operating time of 18 h and a total operating cost of $4,158.83 USD/y. Additionally, it is noted that arrays with the lowest flow rate (2 l/min) take longer to reach the target temperature, resulting in higher pumping costs. On the other hand, arrays with the highest volumetric flow rate of 20 l/min per collector have shorter operating times but experience significant pressure drops, leading to elevated costs.

Table 2: Operating costs of different network structures. Results considering fouling.

Arrangement	$\dot{V}$ (l/min)	ΔP (kPa)	Cost_colec (USD/y)	Cost_pump (USD/y)	Cost_Total (USD/y)	Q (kWh/y)	Cost_Q (kWh)	Operation time (h)	Batches/y	Cost per batch (USD)
8Lx5p	2	937.3	3,247.06	4,290.86	7,537.92	163,020	0.0462	27.09	106	70.90
10Lx 2p-2s	4	1466.6	3,247.06	5,107.94	8,355.00	163,020	0.0513	20.61	140	59.79
4Lx5p-2s	4	1466.6	3,247.06	5,107.94	8,355.00	163,020	0.0513	20.61	140	59.79
5Lx8p	2	937.3	3,247.06	4,290.86	7,537.92	163,020	0.0462	27.09	106	70.90
4Lx2p-5s	10	996.7	3,247.06	2,876.79	6,123.85	163,020	0.0376	17.08	169	36.32
10Lx4p	2	937.3	3,247.06	4,290.86	7,537.92	163,020	0.0462	27.09	106	70.90
10Lx4s	8	1151.7	3,247.06	3,466.25	6,713.31	163,020	0.0412	17.81	162	41.52
8Lx5s	10	996.7	3,247.06	2,848.16	6,095.22	163,020	0.0374	16.91	170	35.79
5Lx8s	16	1543.6	3,247.06	3,837.11	7,084.17	163,020	0.0435	14.71	196	36.18
4Lx10s	20	2340.6	3,247.06	5,584.94	8,832.00	163,020	0.0542	14.12	204	43.30

Based on the time it takes for each arrangement to reach the target temperature, the quantity of batches that can be produced is determined. Considering that the collector field operates 8 h a day, the operation with the original arrangement (4Lx5p-2s) allows for up to 200 batches per year. The arrangement with the shortest operating time can achieve a greater quantity of batches per year (221), while the one with the longest operating time produces a smaller quantity (160 batches per year). However, this result alone is not sufficient to determine which configuration is economically more profitable.

To determine the array that offers the greatest advantages, the unit cost per batch is analysed. This cost per batch directly relates the total cost to the number of batches achievable with each array. The 4Lx2p-5s array yields the lowest unit cost per batch ($18.3). Therefore, it is determined to be the optimal array, considering pumping costs, operating time, and the number of batches achievable.

From the results, it was found that when there is no fouling, the original arrangement 4Lx5p-2s can be reorganised to become an arrangement 4Lx2p-5s to reduce operating costs. While the savings generated from

the total cost are minimal at $21.29 (USD/y), the quantity of batches obtained per year must be considered. If the 4Lx2p-5s arrangement is used to produce the 200 batches per year instead of the original arrangement, the total cost will be $3,660 (USD/y), resulting in an 8% annual savings. On the other hand, if the 8Lx5p arrangement is used to produce the 200 batches, the cost will be $5,200 (USD/year), representing a 30.7% increase compared to the original arrangement. This demonstrates the importance of having an arrangement that generates the lowest cost per batch.

Table 2 presents the results considering fouling effects. Across all arrays, both operating costs and the time required to reach the target temperature increase when fouling is considered, compared to scenarios without fouling. Specifically, for the original array (4Lx5p-2s), the total cost escalates by 52.3% (equivalent to $4,377.77 USD/y), and the operating time extends by 43.4%. Interestingly, in the presence of fouling, the 8Lx5s array becomes the optimal choice. Although it doesn't achieve the shortest time to reach the target temperature, it exhibits the lowest unit cost per batch at $35.79.

4. Conclusions

This study sets the basis for retrofit approaches of existing low-temperature solar collector arrays that operate in batch mode, aiming to enhance energy collection and reduce operating costs. For the case studied in this work, the results indicate that in batch operation of solar flat plate collector fields, configurations with higher volumetric flow rates per collector (such as 5Lx8s, 8Lx5s, and 4Lx10s) achieve the shortest operating time to reach the target temperature. However, these configurations also experience significant pressure drop, resulting in elevated operating costs. On the other hand, arrays with lower volumetric flow rates per collector (8Lx5p, 5Lx8p, and 10Lx4p) exhibit minimal pressure drop but require extended operating times to reach the desired temperature, leading to higher overall costs.

Based on the results, when fouling is not present, it is possible to reduce the operating cost of the solar collector field by modifying the original array (4Lx5p-2s) into a configuration 4Lx2p-5s. The reduction in total cost is minimal ($21.29 USD), but when considering operating time, there is an increase in production of 16 annual batches. When scaling fouling is present, modifying the original array 4Lx5p-2s to the 8Lx5s configuration results in a 27 % decrease in total costs ($2,259.78 USD). Additionally, there is an increase in production of 30 more batches per year (a 21 % increase). In practice, cleaning schemes must be established to prevent scaling from significantly affecting the performance of the solar collector network and increasing operating costs. This work presents the foundations for optimizing the thermal and hydraulic performance of solar collector networks, considering variations in environmental conditions, scaling, alternative heat transfer fluids, and different network arrangements.

References

Arunachala U.C., Bhatt M.S., Sreepathi L.K., 2015, Analytical and Experimental Investigation to Determine the Variation of Hottel–Whillier–Bliss Constants for a Scaled Forced Circulation Flat-Plate Solar Water Heater. Solar Energy Engineering, 137, 051011.

García-Valladares O., Pilatowsky-Figueroa I., Ortiz-Rodríguez N., Menchaca-Valdez C., 2019, Solar thermal dehydrating plant for agricultural products installed in Zacatecas, México. WEENTECH Proceedings in Energy, 5, 01-19.

Koussa M., Saheb D., Belkhamsa H., Lalaoui M.A., Hakem S.A., Sami S., Zoubir B., Mustapha H., 2015, Effect of parallel and serie connection configuration of solar collector on the solar system performances. IREC2015 The Sixth International Renewable Energy Congress, Sousse, Tunisia.1-6.

Lugo-Granados H., Canizalez-Dávalos L., Picón-Núñez M., 2023, Thermohydraulic Effects of Scaling in Flat Plate Solar Collector Networks. Chemical Engineering Transactions, 61, 799-804.

Lugo-Granados H., Picón-Núñez M., 2017, Scaling Growth in Heat Transfer Surfaces and Its Thermohydraulic Effect Upon the Performance of Cooling Systems. Chemical Engineering Transactions, 103, 421-426

Rashed E.S., Ahmed Elsamni O., Elkaranshawy H.A., Elsheniti M.B., 2021, Design and Performance Evaluation of Large Field of Flat Plate Solar Collectors Network for Industrial Application, 12th International Renewable Engineering Conference (IREC), Amman, Jordan, 1-7.

Scolana S., Serrab S., Sochard S., Delmasa P., Reneaume J.M., 2020, Dynamic optimization of the operation of a solar thermal plant. Solar Energy, 198, 643–657.

Shrestha N.L., Frotscher O., Urbaneck T., Oppelt T., Göschel T., Uhlig U., Frey H., 2018, Thermal and hydraulic investigation of large-scale solar collector field. Energy Procedia, 149, 605-614.

Stanciu C., Stanciu D., Ioniţă C., Olaru D.M., 2020, Solar collectors network map: shape and time dynamics of stored thermal energy for different user loads. 9th International Conference on Thermal Equipments, Renewable Energy and Rural Development, 180, 02011.